A $5.8\,\mathrm{GHz}$ Fully-Tunnel-Diodes-Based $20\,\mu\mathrm{W}$, $88\,\mathrm{mV}$, and $48\,\mathrm{dB}$-Gain Fully-Passive Backscattering RFID Tag

Aline Eid, Jimmy Hester, and Manos M. Tentzeris
School of Electrical and Computer Engineering, Georgia Institute of Technology, Atlanta, GA, USA.

***Abstract*— Backscatter front-ends are generally praised for their sub-$\mu\mathrm{W}$ power consumptions. However, this power consumption ends up being dwarfed by that of its modulating baseband circuitry. Furthermore, they are plagued by short reading ranges. The work reported in this paper demonstrates, for the first time, the use of a combined single-element oscillator/reflection-amplifier architecture. This remarkable system combines two critical features for range extension–the highest reflection-amplification RFID gain of the literature $(48\,\mathrm{dB})$ and higher-than-MHz sub-carrier offset frequency–while displaying a power consumption lower than that of any comparable commercial (amplifier-less) oscillator: $20\,\mu\mathrm{W}$. This is achieved by using a tunnel-diode, whose properties as a baseband-oscillator and a $5.8\,\mathrm{GHz}$ reflection-amplifier are analyzed, before both are combined. This highly voltage-sensitive system is synergistically associated with a first-of-a-kind self-regulating tunnel diode-based rectifier to propose a fully-tunnel-diodes-based passive RFID design which could enable the future of practical km-range RFIDs.**

***Keywords*— RFID, backscattering, Internet of Things, energy harvesting, tunnel diode, negative differential resistance.**

I. Introduction

Internet of Things (IoT) devices currently employ active wireless architectures, whose power consumption levels exceed $5\,\mathrm{mW}$ (typical Bluetooth Low Energy (BLE) during emission) and, therefore, are required to put themselves under heavy duty-cycling regimes. Backscatter communications, ubiquitous in the RFID world, offer a single-digit-µW-operating alternative but have paled in comparison to the range offered by active alternatives. This work adds its contribution to a middle-range solution–amplified backscatter–which provides a middle ground between the two aforementioned approaches.

The magnitude of the signal generated by a backscatter modulator is proportional to the modulation factor M defined in Eq. (1) which, for passive front-ends, is always smaller than 1.

$$M = \frac{1}{4}|\Gamma_1 - \Gamma_2|^2 \tag{1}$$

where Γ_1 and Γ_2 are the reflection coefficients at the two extreme states of modulation. With active front-ends comes the ability to create reflection coefficients greater than unity and to, therefore, significantly increase M [1]. This can be achieved using electronic devices that display a negative resistance, and can thus operate as reflection amplifiers under specific biasing conditions. Recent work has demonstrated the implementation of tunnel diodes to achieve the advantageous combination of sub-mW power consumption and reflection gains in excess of $40\,\mathrm{dB}$ [2]. A tunnel diode's behavior is governed by the quantum tunneling effect that results in a unique IV curve that offers a wide range of functions depending on the region where it is being operated. At zero-bias, the diode can be used for harvesting applications. In the negative differential resistance region, the diode can be used as an oscillator or a reflection amplifier. For large biases, the tunnel diode behaves like a Schottky diode and can be implemented in mixer applications. Backscatter systems require the use of a sub-carrier-generating oscillator operating at a frequency high enough to isolate the backscatter signal from the phase-noise-generated reader self-interference (TX to RX). To reach sub-carriers in excess of several MHz, several hundred microwatts of power and dedicated components are currently required.

In this work, and for the first time, three major functions of a tunnel diode are combined together to form a self-sufficient, extremely low-voltage and low power-consumption RFID backscattering system operating within the $5.8\,\mathrm{GHz}$ ISM band, as presented in the schematic of Fig. 1. A self-regulating tunnel diode-based rectifier–that can operate within a radius of more than $3\,\mathrm{m}$ around a $36\,\mathrm{dBm}$ EIRP power source–harvests power at $900\,\mathrm{MHz}$ to bias a tunnel diode-based combined oscillator/reflection amplifier system that enables return gains up to $48\,\mathrm{dB}$ while consuming power as low as $20\,\mu\mathrm{W}$. This system relies only on two tunnel diodes and few passive components to achieve all the requirements for an energy autonomous RFID tag.

II. $5.8\,\mathrm{GHz}$ Tunnel-Diode Basic RFID Tag Elements

A. *Tunnel Diode As an Oscillator*

Tunnel diodes are very promising devices for oscillator circuits up to mm-wave frequencies because they are not limited by transit-time effects. When connected to a simple LC circuit and biased with a voltage that brings its current into the negative resistance region, the resistance losses of the LC circuit could be compensated for by the negative resistance generated by the diode: a necessary condition for stable oscil-

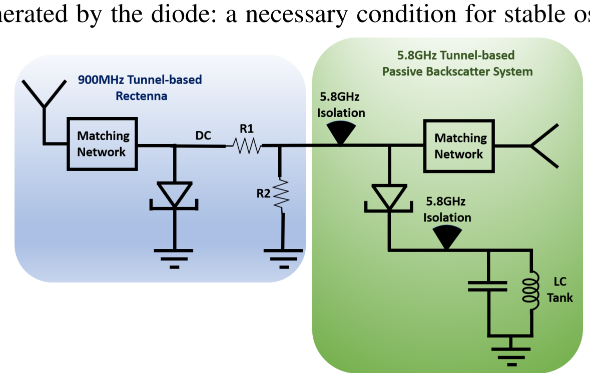

Fig. 1. Schematic of the fully-tunnel-diodes-based passive backscatter tag.

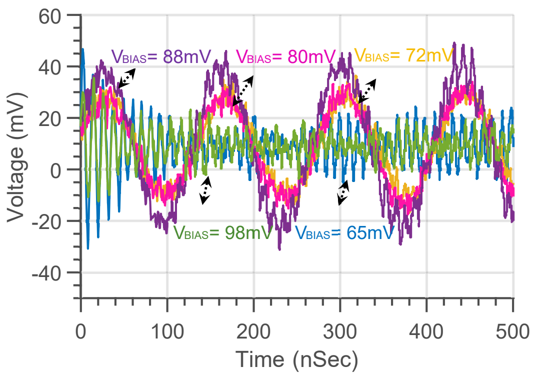

Fig. 2. Measured oscillations for the tunnel diode-based oscillator for different biasing conditions.

lations. Compared to the low power oscillators available in the market, such as the CSS555 micro-power timer or the micro-power oscillators from SiTime, the tunnel diode offers both lower power consumption–with, notably, a biasing voltage down to $70\,\mathrm{mV}$ relative to the $1.2\,\mathrm{V}$ of the aforementioned components–and higher oscillation frequencies in excess of $10\,\mathrm{GHz}$. Finally–as will be shown in the next section–if a diode is used in this mode, it can double as a reflection amplifier without requiring any more biasing power. In this work, the MBD2057-E28X tunnel diode from Aeroflex was connected in series with an LC tank composed of a $0.5\,\mu\mathrm{H}$ inductor with an internal resistance of $31\,\mathrm{m}\Omega$ and a $1\,\mathrm{nF}$ capacitor, that would result in a resonance frequency around $7\,\mathrm{MHz}$. The diode was designed and simulated using Keysight Advanced Design System (ADS), by implementing the non-linear model of the diode extracted from its IV curve and a characterization presented in [3]. For an operation within the negative differential resistance region, a voltage ranging between $70\,\mathrm{mV}$ and $180\,\mathrm{mV}$ is required across the diode. An external voltage source of $0.2\,\mathrm{V}$ was used for this test, accompanied with a set of two resistors for voltage division, to set the proper biasing for the diode and proper current level for the tank circuit. Fig. 2 presents the result of the test of the tunnel diode-based oscillator circuit for different biasing conditions. The power consumption on the diode was measured to be $19\,\mu\mathrm{W}$. It can be seen that the MBD2057 is highly sensitive to the applied voltage and oscillations at the desired frequency occur only for a biasing between $70\,\mathrm{mV}$ and $92\,\mathrm{mV}$.

B. Tunnel Diode As a Reflection Amplifier

The negative resistance resulting in a modulation factor M>1 displayed by the tunnel diode is extremely desirable to extend the range achieved by backscatter modulation systems. This subsection presents the design, fabrication and testing of the $5.8\,\mathrm{GHz}$ MBD2057-based reflection amplifier. The circuit was printed on copper-clad Rogers RO4003C substrate ($\varepsilon r = 3.55$ and $h = 0.508\,\mathrm{mm}$) using an inkjet-printed masking technique followed by etching. Similar to the tunnel diode-based oscillator circuit presented in Sec. II-A, the reflection amplifier was first characterized with respect to the applied biasing voltages. The changes in the amplitude and phase of the reflection coefficients Γ were measured and presented in Fig. 3 for an input power of $-75\,\mathrm{dBm}$ and a frequency of $5.8\,\mathrm{GHz}$. The left side of Fig. 3 contains all the tests results where the biasing voltage was swept over the entire negative resistance region, with amplitudes of Γ exceeding 200. The figure to the right focuses on the region inside the black circle that contains data for reflection coefficients up to an amplitude of 5. The reflection amplifier is then capable of producing reflection coefficients oscillating between $-10\,\mathrm{dB}$ and $48\,\mathrm{dB}$, thereby yielding a modulation factor $M = 11000$. The reflection amplifier is also less sensitive to the changes in biasing voltages compared to the oscillator circuit.

The return gains of the MBD2057-based reflection amplifier were also characterized with respect to changes in RF input powers under the optimal biasing voltage of $120\,\mathrm{mV}$. Fig. 4 presents the excellent behavior of the reflection amplifier, reflecting a gain as high as $51\,\mathrm{dB}$ for an extremely low input power of $-110\,\mathrm{dBm}$. The photo of the fabricated MBD-based reflection amplifier is also presented in Fig. 4. The circuit is composed of the tunnel diode placed in shunt, followed by a short shunt stub for matching and a radial stub for RF isolation. Similar to the previous test with the oscillator, the biasing circuit relied on an external voltage source of $0.2\,\mathrm{V}$ and two variable resistors to enable a tunable biasing voltage on the diode. The power consumption on the diode was measured to be $18\,\mu\mathrm{W}$.

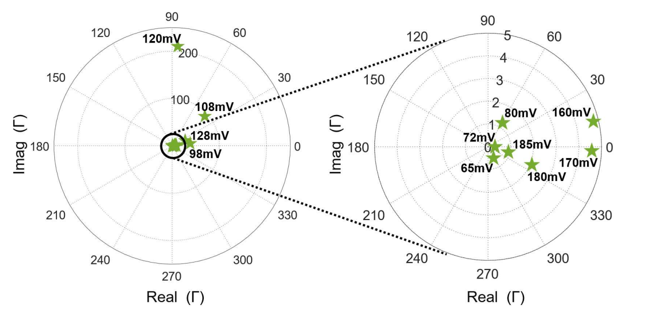

Fig. 3. Measured reflection coefficients Γ (real and imaginary components) for the reflection amplifier for different biasing voltages for an RF signal input power $-75\,\mathrm{dBm}$ and a frequency of $5.8\,\mathrm{GHz}$.

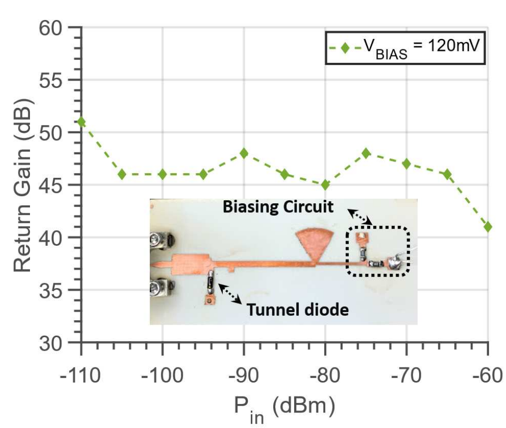

Fig. 4. Measured return gains for the reflection amplifier with respect to RF input powers for a biasing voltage of $120\,\mathrm{mV}$ and a frequency of $5.8\,\mathrm{GHz}$.

C. *Tunnel Diode As a Rectifier*

The previous experiments demonstrating the capabilities of the tunnel diode to operate as an oscillator and a reflection amplifier have also highlighted the importance of a strictly-controlled biasing voltage. This section studies the behavior of the tunnel diode as a rectifier and its suitability as a power source for this system. This was motivated by the fact that its IV curve suggests a rectifying saturation voltage close to that needed to bias this system. As mentioned in the introduction, the tunnel diode can be used for harvesting applications when zero-biased. The circuit presented in Fig. 5 shows the fabricated rectifier using a tunnel diode connected in a shunt configuration, preceded by a meandered-lines-based matching network for miniaturization purposes, and followed by an RF choke. The rectifier is designed at $900\,\mathrm{MHz}$, where up to $36\,\mathrm{dBm}$ EIRP is allowed. The output voltage plotted with respect to the RF input power for different load values shows that the tunnel diode is the perfect power source for the system. The reason behind this perfect match, is that the tunnel diode-based rectifier saturates at a low voltage level, around $0.2\,\mathrm{V}$. Furthermore, it is interestingly remarkably independent on large changes in load values. These characteristics are very different in typical Schottky diodes, a very common choice for harvesting applications, where the diode saturates at much higher voltage levels when it reaches breakdown, in addition to the diode being very sensitive to load changes. The tunnel diode-based rectifier is very suitable for the application presented in this work, where its self-regulating feature above a certain power level will keep the system within its intended operating range, while minimizing the amount of power wasted in dc-dc conversion.

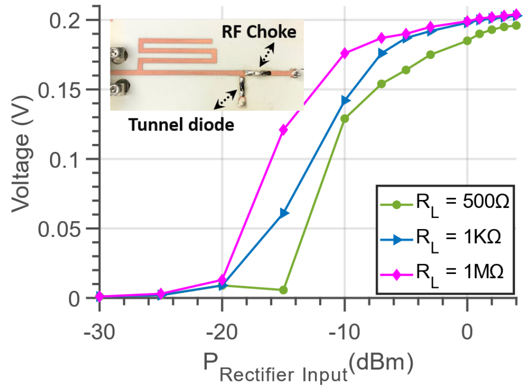

Fig. 5. Measured output voltages for the tunnel diode-based rectifier versus RF input powers for different load conditions.

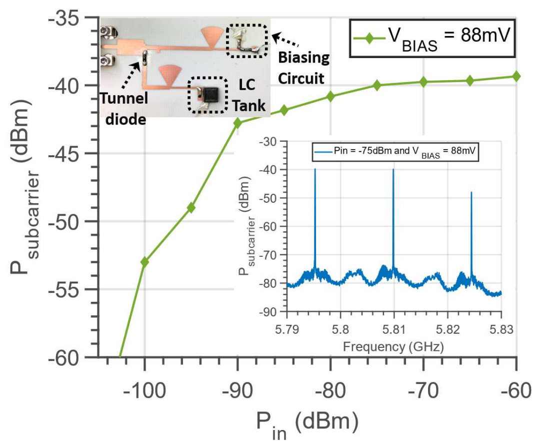

Fig. 6. Fabricated combined oscillator/reflection amplifier system on RO4003C with the measured sub-carrier powers over a range of RF input powers in addition to the display of the modulated and amplified RF signal for P_{in} = $-75\,\mathrm{dBm}$.

III. Fully-Tunnel-Diodes-Based Passive Backscatter System

A. *Single Tunnel Diode with Dual Functions*

Sec. II presented the ability of the tunnel diode in executing separate jobs. Instead of using two separate diodes to achieve an amplified modulated signal, this subsection combines the two functionalities presented in Sec. II-A and Sec. II-B in a single diode following the system presented in Fig. 6. Using a single biasing source and a single diode and by properly placing radial stubs for RF isolation between the tunnel diode and the DC power source from one side and the $7\,\mathrm{MHz}$ oscillation on the other, this system is able to achieve a dual functionality while not consuming additional power. In order to test the behavior of this system, a common biasing voltage point was chosen; more specifically, a choice obeying the high sensitivity of the tunnel diode based-oscillator observed in Sec. II-A. For this purpose, $88\,\mathrm{mV}$ was used to bias the diode at a frequency of $5.8\,\mathrm{GHz}$, while the reflected sub-carrier power was measured for an input power ranging from $-105\,\mathrm{dBm}$ to $-60\,\mathrm{dBm}$. The results prove the successful implementation of the dual functionalities through the use of a single diode with a single bias, with a resulting gain ranging between $21\,\mathrm{dB}$ and $48\,\mathrm{dB}$. Added on top of this plot is a measurement extracted from the spectrum analyzer, showing the amplified modulated signals at the designed oscillating frequency of $7\,\mathrm{MHz}$ surrounding the carrier signal for an input power of $-75\,\mathrm{dBm}$. The power consumption on the diode was measured to be $20\,\mu\mathrm{W}$.

B. *Tunnel-diode-Powered System*

The third capability described in Sec. II-C was then added to the system using a separate diode to provide the proper biasing to the combined oscillator/reflection amplifier system presented in Sec. III-A. In order to test the behavior of the system in a wireless environment, a monopole antenna was designed at $900\,\mathrm{MHz}$ to act as the harvesting receiving antenna that will channel the RF power to the tunnel diode-based rectifier. The size of the antenna can be reduced by more than 50% by applying miniaturization techniques such as meandered lines or meta-material loading, however a simple monopole was used in this work for validation purposes only. On the backscatter front-end side, a patch antenna was designed at $5.8\,\mathrm{GHz}$ to act as the receiver element in the designed tag. Both antennas were cross-polarized to avoid mixing products. Fig. 7a shows the experimental setup used to test the variation in the output powers of the sub-carrier with respect to changes in the distance between the 900 MHz energy harvesting source and the tag, that translates to changes in the RF power at the input of the rectifier. A horn antenna transmitting 36 dBm EIRP at 900 MHz was placed 3 m away from the tag, presented in detail in Fig. 7a to the right. Two horn antennas, acting as the TX and RX for the backscatter communications at 5.8 GHz, were placed at the same distance away from the tag. Since the tunnel diode-based rectifier is self-regulating and saturates at a voltage of around 0.2 V with a slight dependence on the load attached to it, it offers a high level of freedom and flexibility with regards to the location of the tag. This hypothesis is validated in the plot shown in Fig. 7b. The system starts oscillating and amplifying when the RF power at the input of the rectifier is around −5 dBm, corresponding to a distance of 4 m away from the source, under 36 dBm EIRP, considering a transmitter antenna gain of 5 dB and a receiver antenna gain of 2 dB. The operation of the system remains relatively stable as seen in Fig. 7b, with the increase of the power at the input of the rectifier, due to the unique self-regulating feature of the tunnel diode-based rectifier. A 10 dBm increase in the input power did not derail the biasing applied on the tunnel diode-based combined oscillator/reflection amplifier, even with a limited working oscillator voltage range of 70 mV to 92 mV. This experiment entails that in addition to the tunnel diode being able to power the voltage-sensitive tag, it is also providing movement freedom over a wide range of more than 3 m in which the source or receiver could be moved while the system is still able to send amplified modulated signals. In table 1, the striking performance of the proposed system is displayed, highlighted by the highest reflection-amplification RFID gain of the literature and higher-than-MHz sub-carrier offset frequency–while displaying a power consumption lower than that of any comparable commercial (amplifier-less) oscillator.

IV. Conclusion

The work reported in this paper extends landmark efforts demonstrating tunnel-diode-based reflection-amplifier for range extension by improving their performance as reflection amplifiers while significantly cutting down baseband-circuitry power consumption and concomitantly offering a solution to handle their high voltage-sensitivity. With such practicality-boundaries overcome, the reported architecture sets a robust basis for the advent of tunnel-diodes-based fully-integrated, long-range, and ultra-low-power backscattering RFID systems for IoT, wearables and smart agriculture applications.

Table 1. Performance Comparison

Ref.	Gain (dB)	V_{Bias} (V)	Power (μW)	Oscillator	Sub-Carrier Freq. (MHz)
This work 5.8 GHz	48	0.088	20	Included	7
[4] 5.25 GHz	13	2.5	2000	External	NA
[2] 5.8 GHz	40	0.09	45	External	NA
[5] 28 GHz	0	1.5	216	Included	1.4
[6] 868 MHz	0	1.2	2.62	Included	0.034

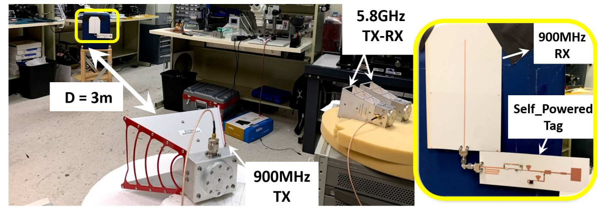

(a)

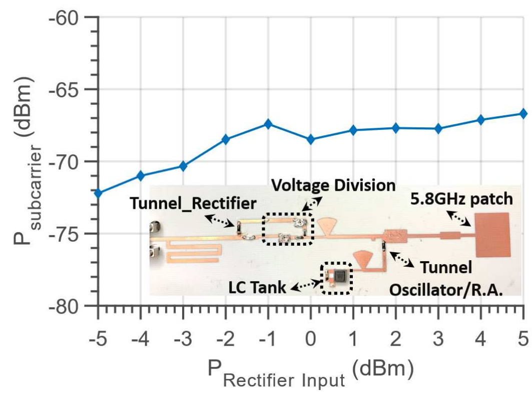

(b)

Fig. 7. (a) Picture of the setup used to measure the sub-carrier output powers with respect to changes in the distance away from the 900 MHz energy source with a photo to the right showing in detail the self-powered tag (b) Measured sub-carrier powers over a range of RF powers at the input of the rectifier in addition to a photo of the fabricated dual tunnel diodes system.

Acknowledgment

The authors would like to acknowledge the support of the Air Force for this work. Also, the authors would like to acknowledge Jo Bito for providing council on some aspects of the system.

References

[1] J. Kimionis, A. Georgiadis, S. Kim, A. Collado, K. Niotaki, and M. M. Tentzeris, "An enhanced-range rfid tag using an ambient energy powered reflection amplifier," in *2014 IEEE MTT-S International Microwave Symposium (IMS2014)*. IEEE, 2014, pp. 1–4.

[2] F. Amato, C. W. Peterson, B. P. Degnan, and G. D. Durgin, "Tunneling rfid tags for long-range and low-power microwave applications," *IEEE Journal of Radio Frequency Identification*, vol. 2, no. 2, pp. 93–103, 2018.

[3] T.-H. Lin, A. Eid, J. Hester, B. Tehrani, J. Bito, and M. M. Tentzeris, "Novel additively manufactured packaging approaches for 5g/mm-wave wireless modules," in *2019 IEEE 69th Electronic Components and Technology Conference (ECTC)*. IEEE, 2019, pp. 896–902.

[4] P. Chan and V. Fusco, "Full duplex reflection amplifier tag," *IET Microwaves, Antennas & Propagation*, vol. 7, no. 6, pp. 415–420, 2013.

[5] J. G. Hester and M. M. Tentzeris, "A mm-wave ultra-long-range energy-autonomous printed rfid-enabled van-atta wireless sensor: At the crossroads of 5g and iot," in *Microwave Symposium (IMS), 2017 IEEE MTT-S International*. IEEE, 2017, pp. 1557–1560.

[6] S. N. Daskalakis, G. Goussetis, S. D. Assimonis, M. M. Tentzeris, and A. Georgiadis, "A uw backscatter-morse-leaf sensor for low-power agricultural wireless sensor networks," *IEEE Sensors Journal*, vol. 18, no. 19, pp. 7889–7898, 2018.